Available online at www.sciencedirect.com
SCIENCE DIRECT
Polymer 47 (2006) 1397–1404
polymer
www.elsevier.com/locate/polymer

The electronic structure and optical properties of carbazole-based conjugated oligomers and polymers: A theoretical investigation

Li Yang [a], Ji-Kang Feng [a,b,*], Ai-Min Ren [a], Jia-Zhong Sun [a]

[a] State Key Laboratory of Theoretical and Computational Chemistry, Institute of Theoretical Chemistry, Jilin University, Changchun 130023, China
[b] College of Chemistry, Jilin University, Changchun 130023, China

Received 26 October 2005; received in revised form 16 December 2005; accepted 16 December 2005
Available online 10 January 2006

Abstract

The application of polyfluorenes (PFs) in polymeric light-emitting diodes (PLEDs) has been hampered because of the charge injection difficulties and the troublesome formation of a tailed emission band at long wavelengths (>500 nm) during device fabrication and operation, leading to both a color instability and reduced efficiency. The polycarbazoles have been proved to efficiently suppress the keto defect emission. In this contribution, we apply quantum-chemical techniques to investigate poly(*N*-methyl-2,7-carbazolediyl) (PCz), and its copolymers poly(*N*-methyl-2,7-carbazolediyl-alt-2,5-thiophene) (PCzT) and poly(*N*-methyl-2,7-carbazoleethynylene) (PCzE), and gain a detailed understanding of the influence of carbazole units and the introduction of different charge carriers on the electronic and optical properties. The electronic properties of the neutral molecules, HOMO–LUMO gaps (Δ_{H-L}), in addition to IPs and EAs, are studied using B3LYP functional. The lowest excitation energies (E_gs) and the maximal absorption wavelength λ_{abs} are studied employing the time dependent density functional theory (TDDFT). The calculated results show that the HOMO energies lift about 0.3 eV and thus the IPs decrease about 0.3 eV in all the carbazole-based polymers, suggesting the significant improved hole-accepting and transporting abilities. More important, by introducing the charge carriers thiophene ring and ethynylene, the LUMO energies in PCzT and PCzE decrease around 0.4 and 0.6 eV, respectively, which contributes to the decreasing EAs and the consequent improved electron-accepting and transporting properties. In addition, the energy gap tends to narrow and the absorption and emission peaks are gradually red-shifted to longer wavelengths with an increase in chain planarity in the copolymers.

Keywords: Carbazole; Optical; DFT

1. Introduction

Recently, more attention has been paid to polyfluorenes (PFs) [1–6] for use as the emissive layer of blue-emitting diodes because of their high photoluminescence (PL) quantum efficiency, thermal stability, and also their facile color tunablility, which can be obtained by introducing low-band-gap comonomers [7–9]. However, blue-light-emitting polyfluorenes show a tailed emission band at long wavelengths (>500 nm) during device fabrication and operation, leading to both a color instability and reduced efficiency. These were initially assigned to the undesired interchain aggregation and/or excimer formation of the polymer chain [10], but more recently it has been shown that the emission from PFs arises from emissive fluorenone defects formed by oxidation at the methane bridge [11]. Another serious problem associated with polyfluorene homopolymer is the significant energy barrier for hole or electron injection and transport with the currently available anode and cathode materials [12].

Synthesis and investigation of new conjugated polymers are essential to improving the electronic and optoelectronic properties of these materials and in turn improvement of the performance of the devices. One approach to address the deficiency is the modification of chemical structures through the incorporation of charge carriers in to the polymer backbone. Recently, 2,7-carbazole derivatives have been synthesized [13–15]. Poly(2,7-carbazole) derivatives are a particularly suitable class of materials for applications in light-emitting devices with the advantages of emitting in the blue region of the visible spectrum, chemical and photochemical stability in air, and the high purity. This is because carbazole contains a rigid biphenyl unit (which leads to a large band gap with efficient blue emission) and the facile substitution at

* Corresponding author. Address: State Key Laboratory of Theoretical and Computational Chemistry, Institute of Theoretical Chemistry, Jilin University, 119 JieFang Road, Changchun 130023, China. Tel.: +86 431 8499856; fax: +86 431 8498026.
E-mail address: jikangf@yahoo.com (J.-K. Feng).

0032-3861/$ - see front matter © 2006 Elsevier Ltd. All rights reserved.
doi:10.1016/j.polymer.2005.12.065

the remote N-position provides the possibility of improving the solubility and processability of polymers without significantly increasing the steric interactions in the polymer backbone. Most interestingly, this class of materials is not subject to the formation of ketone defects.

In this paper, carbazole serves as the main conjugated-backbone. Its polymer and the copolymer with charge carrier thiophene and ethynylene have been investigated in experiment [14,15], which raises a way to design the copolymers with enhanced hole injection and negligible low-energy emission band by modifying the chemical structures. Here, we further explore the ground and low-lying excited states of polymers poly(*N*-methyl-2,7-carbazolediyl) (PCz), poly(*N*-methyl-2,7-carbazolediyl-alt-2,5-thiophene) (PCzT) and poly(*N*-methyl-2,7-carbazoleethynylene) (PCzE) [15] by theoretical studies. Then we apply the experimentally well-known reciprocal rule for polymers, which states that many properties of homopolymers tend to vary linearly as functions of reciprocal chain lengths [16–27]. A distinct advantage of this approach is that it can provide the convergence behavior of the structural and electronic properties of oligomers. In this paper, the ground states of all the oligomers will be treated using the B3LYP functional, and the low-lying excited states will be examined using time-dependent DFT (TDDFT). The energy gap has been estimated from two ways, namely, HOMO–LUMO gaps and the lowest excited energies. Highly conjugated poly(*N*-substituted-2,7-carbazole)s should lead to optimized electrical and optical properties and should shed some light on the structure–property relationships in this class of materials. We were particularly interested in exploring the structural properties of carbazole and the influence of different charge carriers on electronic materials.

2. Computational details

All calculations on these oligomers studied in this work have been performed on the SGI origin 2000 server using Gaussian 03 program package [28]. Calculations on the electronic ground state were carried out using density functional theory (DFT), B3LYP/6-31G*. The investigated polymers $(Cz)_n$, $(CzT)_n$ and $(CzE)_n$ (as depicted in Fig. 1) correspond to copolymers in literature [15], and the main difference is that the oligomers under study substitute octyl or 2-ethylhexyl with methyl at 9-position in carbazole, for the sake of reducing the time of calculation.

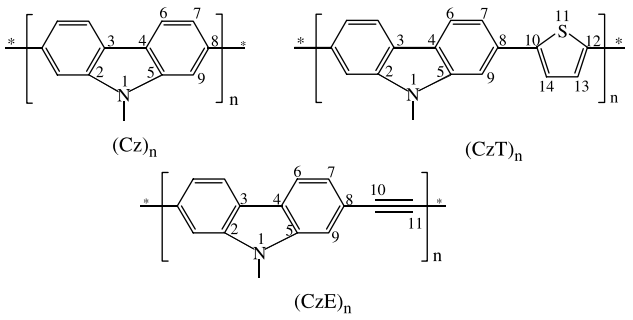

Fig. 1. The sketch map of the structures.

As already mentioned before, one of the most important features of the π-conjugated polymers is their ability to become highly conducting after oxidative (p-type) or reductive (n-type) [19] doping. So, single point calculations are carried out to obtain the ionization potentials (IPs) and electron affinities (EAs). The energy gap has been estimated from two ways, namely, HOMO–LUMO gaps and the lowest excited energies. We employed the linear extrapolation technique in this research, which has been successfully employed to investigate several series of polymers [23–27,29–31]. The nature and the energy of the first eight singlet–singlet electronic transitions have been obtained by TDDFT/B3LYP calculations performed on the B3LYP/6-31G* optimized geometries, and the results are compared with the available experimental data. The excited geometries were optimized by ab initio CIS/3-21G* [32]. Based on the excited geometries, the emission spectra of monomers and dimers of the three series are investigated.

3. Results and discussion

3.1. Ground states structural properties

The results of the optimized structures for the copolymeric molecules of the PCz, PCzT and PCzE show that the carbazole has the similar conformation in the three series (as depicted in Fig. 2). Because the dihedral angle between two phenyl rings in carbazole is fixed by ring bridged-atoms which tend to keep their normal tetrahedral angles in their ring linkage, the carbazole keeps their quasi planar conformation and the dihedral angles in them are no more than 1°. The biggest torsional angels in $(Cz)_n$ are the inter-ring torsional angles between the two adjacent carbazole rings. Compared with pristine polyfluorene in which the inter-ring torsional angle is ∼36° [27], a slightly large twisted angle is observed in PCz (∼38°), in the other word, the π-conjugated backbone in $(Cz)_n$ is broken. However, the introduction of charge carriers into carbazole enhances the π-conjugated structures. The ground-state geometry of each oligomer in $(CzT)_n$ is less twisted than that in $(Cz)_n$ and the inter-ring dihedral angels between carbazole and thiophene are around 27°, due to the strong push-pull effect between the carbazole ring and the thiophene ring, which thus leading to the slightly shorter inter-ring distances than $(Cz)_n$. The $(CzE)_n$ sequence has the fully planar conformation with the dihedral angels almost 0°, due to the incorporation with highly planar charge carrier ethynylene. Accordingly, the inter-ring distances are the shortest.

3.2. Frontier molecular orbitals

It will be useful to examine the highest occupied orbitals and the lowest virtual orbitals for these oligomers and polymers because the relative ordering of the occupied and virtual orbitals provides a reasonable qualitative indication of the subsequent excitation properties [33] and of the ability of

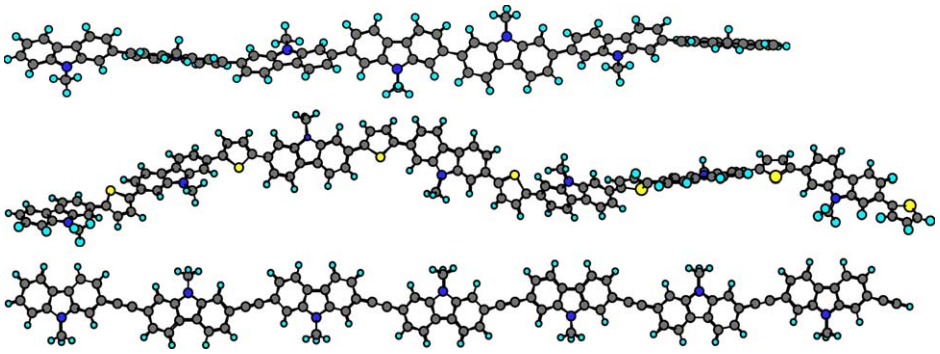

Fig. 2. Optimized structures of $(Cz)_7$ (top), $(CzT)_7$ (middle) and $(CzE)_7$ (bottom).

electron or hole transport. The electron density isocontours of HOMO and LUMO of the oligomers in $(Cz)_n$, $(CzT)_n$ and $(CzE)_n$ ($n=1$–7) by B3LYP/6-31G* are plotted in Fig. 3.

Fig. 3 shows that all frontier orbitals in the oligomers of all series under study spread over the whole π-conjugated backbone. In general, the HOMO possesses an antibonding character between the subunits. This may explain the nonplanarity observed for these oligomers in their ground states. On the other hand, the LUMO of all the oligomers generally shows a bonding character between the subunits. This implies that the singlet excited state involving mainly the promotion of an electron from the HOMO to the LUMO should be more planar.

In experiment, the HOMO and LUMO energies were calculated from one empirical formula proposed by Brédas et al., based on the onset of the oxidation and reduction peaks measured by cyclic voltammetry, assuming the absolute energy level of ferrocene/ferrocenium to be 4.4 eV below vacuum

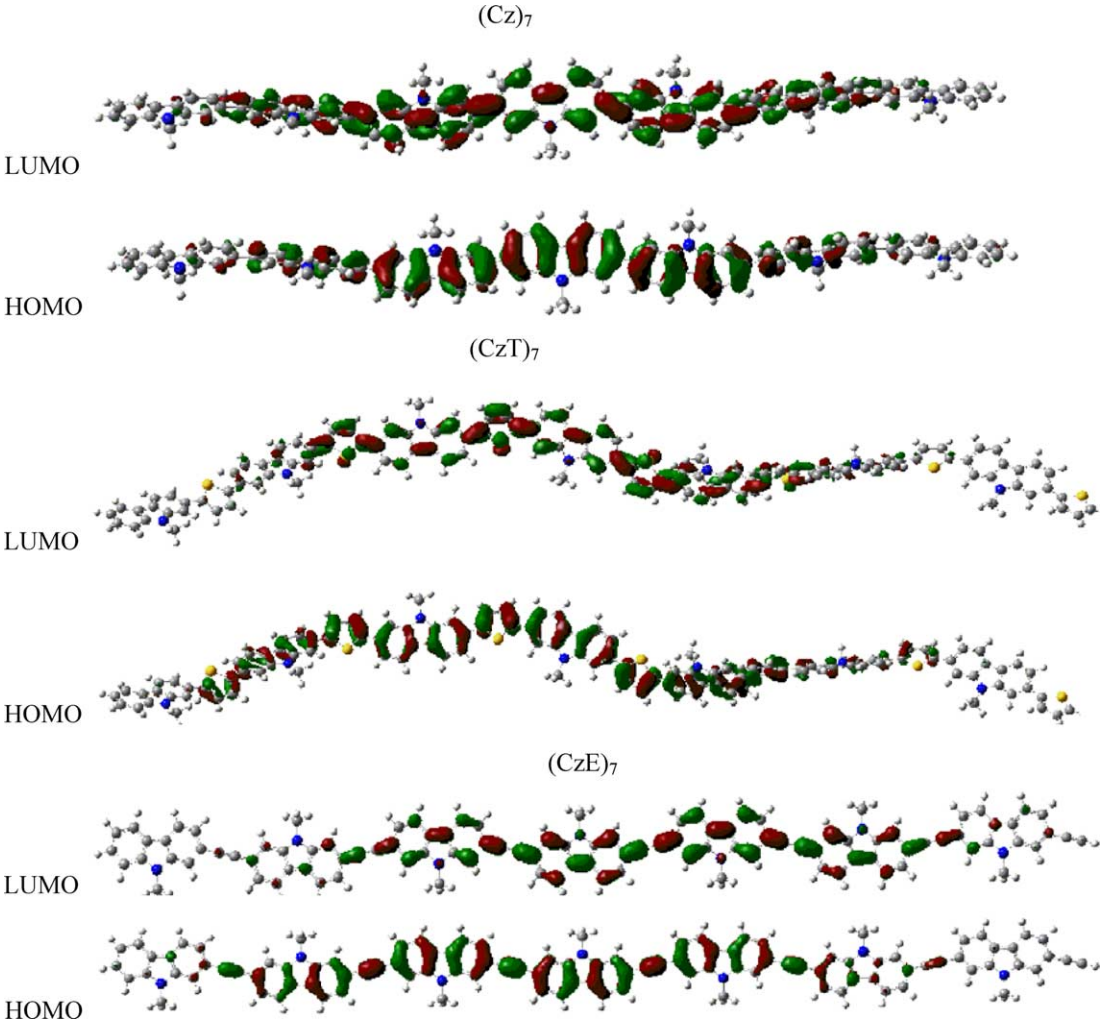

Fig. 3. The HOMO and LUMO orbitals of $(Cz)_n$, $(CzT)_n$ and $(CzE)_n$ ($n=7$) by B3LYP/6-31G*.

Table 1
The negative of HOMO and LUMO energies ($-\varepsilon_{HOMO}$, $-\varepsilon_{LUMO}$)(eV) of $(Cz)_n$, $(CzT)_n$ and $(CzE)_n$ obtained by B3LYP/6-31 G*

Oligomer	$-\varepsilon_{HOMO}$	$-\varepsilon_{LUMO}$
$(Cz)_n$		
$n=1$	5.32	0.62
$n=2$	5.24	1.05
$n=3$	5.10	1.20
$n=4$	5.03	1.28
$n=5$	4.99	1.32
$n=6$	4.97	1.34
$n=7$	4.96	1.35
$(CzT)_n$		
$n=1$	5.34	1.11
$n=2$	4.98	1.52
$n=3$	4.88	1.65
$n=4$	4.86	1.69
$n=5$	4.83	1.70
$n=6$	4.84	1.74
$n=7$	4.83	1.75
$(CzE)_n$		
$n=1$	5.48	1.08
$n=2$	5.15	1.57
$n=3$	5.01	1.74
$n=4$	4.95	1.82
$n=5$	4.92	1.85
$n=6$	4.90	1.87
$n=7$	4.89	1.89

[19], whereas, the HOMO and LUMO energies can be calculated accurately by density functional theory (DFT) in this study. The negative of HOMO energies ($-\varepsilon_{HOMO}$) and LUMO energies ($-\varepsilon_{LUMO}$) of these orbitals in PCz, PCzT and PCzE have been compiled in Table 1.

As is usual in π-conjugated systems, with the increasing conjugation lengths the HOMO energies increase, whereas the LUMO energies decrease in all series. Similar energies are obtained for the HOMO of the longest oligomer of PCzT (∼ −4.83 eV) and PCzE (∼ −4.89 eV) oligomers, which are both slightly higher than that of PCz (∼ −4.96 eV), suggesting that the introduction of electron-donating thiophene unit and the more planar conformation will both slightly lift the HOMO of pristine polycarbazole. In general, the HOMO energies in carbazole-based polymers are higher more than 0.3 eV than that in PF (∼ −5.2 eV) [27] oligomers, indicating the much improved hole-accepting properties, especially by introducing electron-donating moiety thiophene into the carbazole backbone. Turning to the evolution of the LUMO levels, the LUMO of PF (∼ −1.3 eV) [27] is similar to PCz (∼ −1.3 eV), whereas are generally stabilized by about 0.4 and 0.6 eV with respective to PCzT (∼ −1.7 eV) and PCzE (∼ −1.9 eV), respectively. This result indicates that the combination with charge carriers or enlarge the conjugated backbone will both lower the LUMO energies. The more planar conformations in the three series under study relative to PF are also the reasons. Since HOMO shows inter-ring antibonding character and the LUMO shows inter-ring bonding character and the variation of torsional angles should have larger effects on LUMO. Indeed, the decreasing in the dihedral angles between the two adjacent subunits induced by the presence of the electron-donating moiety thiophene or highly planar ethynylene should enhance the electron conjugation over the whole molecule and thus stabilize the LUMOs. The two features allow an efficient electron-accepting/transporting ability.

3.3. Ionization potentials and electron affinities

The adequate and balanced transport of both injected electrons and holes are important in optimizing the performance of OLED devices. The ionization potential (IPs) and electron affinity (EAs) are well-defined properties that can be calculated by DFT to estimate the energy barrier for the injection of both holes and electrons into the polymer. Table 2 contains the ionization potentials (IPs), electron affinities (EAs) (v; at the geometry of the neutral molecule). As a whole, all plotted data do not show a good linearity, however, as shown in Table 2, with the increase of conjugation length, the linearity becomes more obvious. So in order to get the polymeric information, we use the last four points ($n=4$–7) to perform a linearity fitting and extrapolate the linear to the infinite chain length. Fig. 4 displays plots of IPs and EAs as functions of reciprocal chain length for the series of $(Cz)_n$, $(CzT)_n$ and $(CzE)_n$ ($n=1$–7) under study.

One general challenge for the application of polymers in PLEDs is achievement of high electron affinity (n-type) conjugated polymers for improving electron injection/transport and low ionization potential (p-type) conjugated polymers for better hole injection/transport in polymer electronic devices. For PCz, PCzT and PCzE, the energies required to create a hole in the polymers are around 5.16, 5.01 and 5.01 eV,

Table 2
Ionization potentials and electron affinities for each molecular (in eV)

Electron volt	$n=1$	$n=2$	$n=3$	$n=4$	$n=5$	$n=6$	$n=7$	$n=\infty$
$(Cz)_n$								
IP(v)	6.98	6.67	6.22	5.91	5.77	5.68	5.58	5.16
EA(v)	1.03	0.17	0.21	0.41	0.55	0.65	0.72	1.16
$(CzT)_n$								
IP(v)	6.79	6.03	5.72	5.56	5.44	5.39	5.32	5.01
EA(v)	0.30	0.50	0.82	0.97	1.11	1.19	1.25	1.61
$(CzE)_n$								
IP(v)	7.08	6.28	5.92	5.72	5.59	5.50	5.42	5.01
EA(v)	0.47	0.47	0.84	1.04	1.18	1.29	1.34	1.78

The suffixes (v) indicate vertical and adiabatic values.

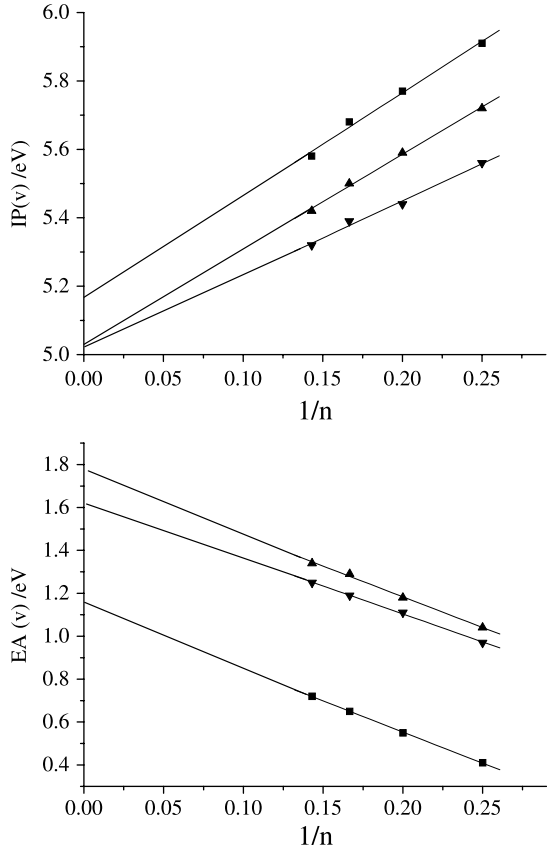

Fig. 4. IP(v)s and EA(s) of $(Cz)_n$, $(CzT)_n$ and $(CzE)_n$ as a function of reciprocal chain length in oligomers.

respectively, which are all lower than that in PF (~5.4 eV) [27], which is consistent with the analysis for HOMO energy. Thus, the hole injection and transportation of carbazole-based polymers are expected to be easier than PF, and as a consequence the charge carrier balance is better in the devices constructed from the copolymers. The extraction of an electron from the anion requires ~1.2 eV in PF [27], which is comparable to PCz (~1.16 eV), whereas largely lower than PCzT (~1.61 eV) and PCzE (~1.78 eV). This indicates that the combination with charge carriers moiety or extending the conjugated backbone will improve the electron-accepting/transporting properties. It is clear from these results that the optoelectronic properties of a conjugated polymer are primarily governed by the chemical structure of the polymer backbone. This should be useful to enhance the injection of holes and electron-transport from anode and cathode in light-emitting diodes.

3.4. HOMO–LUMO gaps and the lowest excitation energies

There are two theoretical approaches for evaluating the energy gap in this paper. One way is based on the ground-state properties, from which the band gap is estimated from the energy difference between the highest occupied molecular orbital (HOMO) and the lowest unoccupied molecular orbital (LUMO) [34–36], when $n=\infty$, termed the HOMO–LUMO gaps (Δ_{H-L}s). The TDDFT, which has been used to study systems of increasing complexity due to its relatively low computational cost and also to include in its formalism the electron correlation effects, is also employed to extrapolate energy gap of polymers from the calculated first dipole-allowed excitation energy of their oligomers. Here, the HOMO–LUMO gaps (Δ_{H-L}s) and lowest singlet excited energies (E_g) are both listed in Table 3 and the relationships between the calculated Δ_{H-L} and the E_g and the inverse chain length are plotted in Fig. 5. As far as the whole trend is concerned, the linearity between them is not perfect. But with the increase of the repeated units, the trend in linearity is observed.

Interestingly, for copolymers studied in this work, good agreements between the HOMO–LUMO gaps and experimental observations have been demonstrated with density functional theory (DFT). Optical band gaps derived from the absorption edge of a polymer thin film for $(Cz)_n$ and $(CzT)_n$ are 3.27 and 2.97 eV [14], differed 0.15 and 0.0 eV, from our calculated values by HOMO–LUMO gap of 3.42 and 2.97 eV, respectively. Despite the good agreement, deviations still exists. Two factors may also be responsible for deviations by both methods from experimental. One is that the predicted band gaps are for the isolated gas-phase chains, while the experimental band gaps are measured in the liquid phase where the environmental influence may be involved. Another is that

Table 3
The HOMO–LUMO gaps (Δ_{H-L}) (eV) by B3LYP and the lowest excitation energies (E_g) (eV) by TDDFT of $(Cz)_n$, $(CzT)_n$ and $(CzE)_n$ ($n=1$–7)

Oligomer	Δ_{H-L}	E_g (TD)
$(Cz)_n$		
$n=1$	4.70	4.17
$n=2$	4.19	3.80
$n=3$	3.90	3.58
$n=4$	3.75	3.42
$n=5$	3.67	3.34
$n=6$	3.63	3.31
$n=7$	3.61	3.27
$n=\infty$	3.42	3.08
Expl.	3.27	
$(CzT)_n$		
$n=1$	4.23	3.81
$n=2$	3.46	3.17
$n=3$	3.23	2.92
$n=4$	3.17	2.86
$n=5$	3.11	2.78
$n=6$	3.10	2.78
$n=7$	3.08	2.75
$n=\infty$	2.97	2.62
Expl.	2.97	
$(CzE)_n$		
$n=1$	4.40	3.96
$n=2$	3.58	3.34
$n=3$	3.27	2.99
$n=4$	3.13	2.84
$n=5$	3.07	2.77
$n=6$	3.03	2.70
$n=7$	3.00	2.63
$n=\infty$	2.85	2.37

Optical band gap derived from the absorption edge of a polymer thin film in Ref. [14].

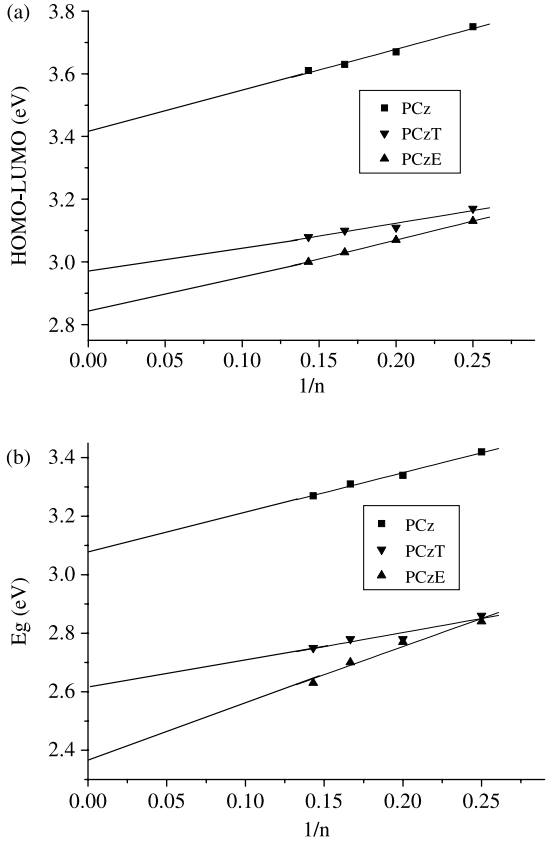

Fig. 5. The HOMO–LUMO gaps by B3LYP and the lowest excitation energies E_gs by TDDFT as a function of reciprocal chain length n in oligomers of $(Cz)_n$, $(CzT)_n$ and $(CzE)_n$.

it should be borne in mind that solid-state effects (like polarization effects and intermolecular packing forces) have been neglected in the calculations [37,38].

Comparing the calculated values of PF with PCz, PCzT and PCzE, we can find the superiority of carbazole-based polymers and the influence of the introduction of charge carriers. The energy gaps obtained by HOMO–LUMO and TDDFT gaps are in 3.42 and 3.08 eV for PCz, which is higher than that 3.33 and 2.91 eV for PF [27] with the same corresponding methods. It can be concluded that the breaking of the conjugation in the backbone induced by carbazole content broadened its energy gap, which also agree well the experimental results. Whereas, the energy gaps in PCzT and PCzE both dramatically lower than that in PCz and PF, which also suggests that electron carriers allow modulate the band gaps and the highly planar conjugated conformation facilitate the decreasing of the energy gaps.

3.5. Absorption spectra

The TDDFT/B3LYP/6-31G* has been used on the basis of the optimized geometry to obtain the nature and the energy of the singlet–singlet electronic transitions of all the oligomers in all series under study as reported in Table 4. All electronic transitions are of the π–π* type and no localized electronic transitions are exhibited among the calculated singlet–singlet transitions. Two interesting trends on the oscillator strength can be observed in all series of oligomers: (1) the oscillator strengths (f) of the lowest $S_0 \rightarrow S_1$ electronic transition are the overwhelmingly largest in all series of oligomers with the repeat units varying from 3 to 7; (2) the oscillator strength coupling the lowest CT π–π* singlet excited state to the ground state increase strongly when going from an isolated molecule to a molecular group and this trend goes along with the conjugation lengths increasing.

Excitation to the S_1 state when $n = 3$–7 corresponds almost exclusively to the promotion of an electron from the HOMO to the LUMO. As in the case of the oscillator strength, the absorption wavelengths arising from $S_0 \rightarrow S_1$ electronic transition increase progressively with the conjugation lengths increasing. It is reasonable, since HOMO→LUMO transition is predominant in $S_0 \rightarrow S_1$ electronic transition and as analysis above that with the extending molecular size, the HOMO–LUMO gaps decrease. It is obvious that the absorption maximum of the longest oligomeric chains exhibit red-shift going from PCz to PCzT and PCzE, which is consistent with the estimation from the energy gap. Since the first allowed transitions are also the absorption maximum, they have the same variation trend.

Table 4
Electronic transition data obtained by the TDDFT/B3LYP/6-31G* for $(Cz)_n$, $(CzT)_n$ and $(CzE)_n$

Electronic transitions	λ_{abs} (nm)	f	Main configurations
$(Cz)_7$			
$S_0 \rightarrow S_1$	379.68	4.74	HOMO→LUMO (0.65)
$S_0 \rightarrow S_4$	341.21	0.07	HOMO-6→LUMO (0.32)
			HOMO-8→LUMO (0.31)
$S_0 \rightarrow S_6$	339.85	0.02	HOMO-10→LUMO (0.47)
			HOMO-6→LUMO (0.23)
$S_0 \rightarrow S_7$	338.29	0.03	HOMO-8→LUMO (0.44)
			HOMO-6→LUMO+1 (0.24)
$S_0 \rightarrow S_8$	338.12	0.01	HOMO-9→LUMO (0.35)
			HOMO-8→LUMO+1 (0.25)
Exp.	380		
$(CzT)_7$			
$S_0 \rightarrow S_1$	451.05	5.95	HOMO→LUMO (0.61)
$S_0 \rightarrow S_2$	429.52	0.48	HOMO-1→LUMO (0.47)
			HOMO→LUMO+1 (0.43)
$S_0 \rightarrow S_3$	410.49	0.06	HOMO-1→LUMO (0.47)
			HOMO→LUMO+1 (0.45)
$S_0 \rightarrow S_4$	406.77	0.90	HOMO-1→LUMO (0.48)
			HOMO-2→LUMO (0.30)
$S_0 \rightarrow S_5$	399.86	0.16	HOMO-2→LUMO (0.57)
			HOMO→LUMO+2 (0.28)
Exp.	419		
$(CzE)_7$			
$S_0 \rightarrow S_1$	471.38	7.96	HOMO→LUMO (0.61)
$S_0 \rightarrow S_3$	415.82	0.09	HOMO→LUMO+1 (0.48)
			HOMO-1→LUMO (0.46)
$S_0 \rightarrow S_4$	406.00	1.19	HOMO-1→LUMO+1 (0.57)
			HOMO-2→LUMO (0.22)
$S_0 \rightarrow S_5$	396.48	0.03	HOMO-2→LUMO (0.62)
$S_0 \rightarrow S_6$	338.12	0.03	HOMO→LUMO+2 (0.60)
Exp.	375		

Absorption wavelengths in chloroform at room temperature in Ref. [15].

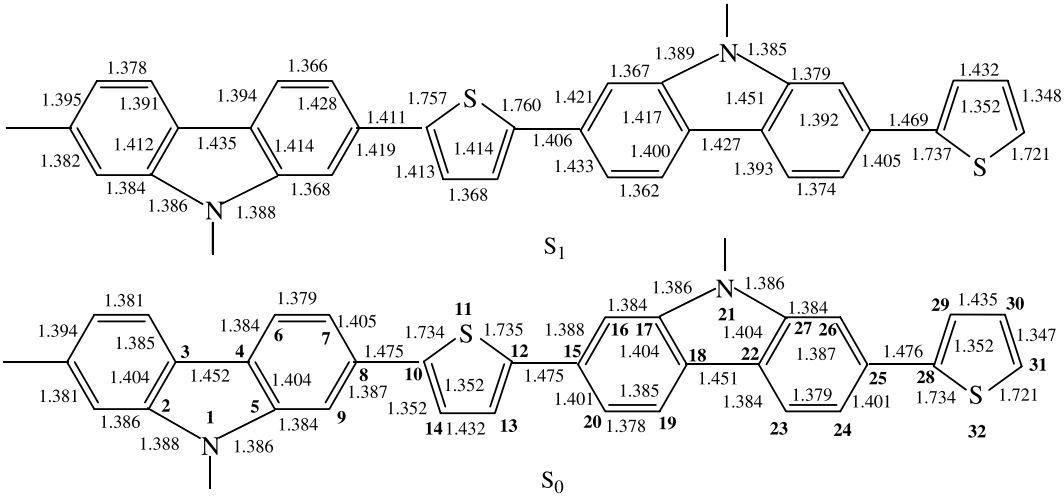

Fig. 6. Comparison of the excited structure (S_1) by CIS/3-21G* with the ground geometry (S_0) by HF/3-21G* of $(CzT)_2$.

3.6. The properties of excited structures and the emission spectra

Up to now, the standard for calculating excited state equilibrium properties of larger molecules is the configuration interaction singles (CIS) method. When paired with a basis set, CIS method can be used to define excited state whose results may be compared across the full range of practical systems. Because the calculation of excited-state properties typically requires significantly more computational effort than is needed for the ground states and dramatically constrains by the size of the molecules, we only optimize the monomer and dimer of each series by CIS/3-21G*. In Fig. 6, we take $(CzT)_2$ as an example to compare the excited structures by CIS/3-21G* with their ground structures by HF/3-21G*. Interestingly, the main characters of the front orbitals by HF/3-21G* are the same to that by B3LYP/6-31G*. As shown, some of the bond lengths lengthened, but some shortened. We can predict the differences of the bond lengths between the ground (S_0) and singlet excited state (S_1) from MO nodal patterns. Due to the singlet state corresponds to an excitation from the HOMO to the LUMO in all considered oligomers, we can explore the bond lengths variation by analyzing the HOMO and LUMO. The HOMO is bonding across the r(2,3), r(4,5), r(4,6), r(7,8), r(8,9), r(10,14), r(12,13), r(15,16), r(15,20), r(17,18), r(18,19), r(22,27), r(22,23), r(24,25), and r(25,26) bonds in $(CzT)_2$, but the LUMO has nodes in these regions. Therefore, one would expect elongation of these bonds; the data in the figure shows that these bonds are in fact considerably longer in the excited state. The HOMO has a node across the r(3,4), r(6,7), r(5,9), r(8,10), r(13,14), r(12,15), r(16,17), r(19,20), r(18,22), r(26,27) and r(25,28) bonds in $(CzT)_2$, while the LUMO is bonding. The data confirm the anticipated contraction of these bonds.

The dihedral angles Φ(7,8,10,11), Φ(11,12,15,16) and Φ(26,25,28,29) in $(CzT)_2$ reduced from 42, 41 and 43° by HF/3-21G* to nearly zero degree by CIS/3-21G*, respectively, that is, the r(8,10), r(12,15) and r(25,28) bond rotates during exciting. $(Cz)_2$ is in the similar case with $(CzT)_2$, and $(CzE)_2$ still keep high-planar conformation. It is obvious that the excited structure has a strong coplanar tendency in all the series, in the other word, the conjugation is better in the excited structure, which is in consistent with the estimation from the character of the frontier orbitals.

On the excited geometries optimized by ab initio CIS, the emission wavelengths are computed by TDDFT to monomer and dimer of PCz, PCzT and PCzE and only the emission

Table 5
Electronic transition data obtained by the TDDFT/B3LYP/3-21G* based on the CIS/3-21G* geometries for the monomer and dimer of PCz, PCZT and PCzE

Electronic transitions	Wavelengths (nm)	f	MO/character	Coefficient	Wavelengths exp./nm
$(Cz)_2$					
$S_1 \rightarrow S_0$	376.55	1.5014	HOMO→LUMO	0.63	415[a]
$S_2 \rightarrow S_0$	359.07	0.0003	HOMO-1→LUMO	0.66	
$S_3 \rightarrow S_0$	348.64	0.0651	HOMO-2→LUMO	0.66	
$(CzT)_2$					
$S_1 \rightarrow S_0$	471.47	2.0868	HOMO→LUMO	0.63	467[a]
$S_2 \rightarrow S_0$	388.60	0.0118	HOMO-1→LUMO	0.68	
$S_3 \rightarrow S_0$	385.50	0.0136	HOMO-2→LUMO	0.67	
$(CzE)_2$					
$S_1 \rightarrow S_0$	409.40	2.2218	HOMO→LUMO	0.64	406[a]
$S_2 \rightarrow S_0$	367.35	0.0207	HOMO-1→LUMO	0.67	
$S_3 \rightarrow S_0$	360.90	0.0262	HOMO-2→LUMO	0.66	

[a] Fluorescence wavelengths in chloroform at room temperature [15].

wavelengths of dimers are listed in Table 5. It can be found that the calculated results accord well with the experimental observation [15]. As in the case of the absorption spectra, the emission peaks with strongest oscillator strength in the dimers are all assigned to $\pi\pi^*$ character arising from S_1, HOMO to LUMO transition. However, the fluorescence spectrum of the three series generally exhibits two shoulders, which is different to their absorption counterpart. The absorption does not show any vibronic peaks. This strongly suggests that the three series polymers are more planar in its first relaxed excited state. The dramatic bathochrome in $(CzT)_2$ upon combination with a thiophene ring is attributed to the strong push–pull effect between the carbazole ring and the thiophene ring and an increase of the polymer chain planarity in the excited geometries.

4. Conclusion

A slightly more twisted conformation in PCz is observed compared with pristine PF. However, the introduction of the charge carriers thiophene ring and ethynylene, results in the highly planar conformations. All decisive molecular orbitals are delocalized on all subunits of the oligomers. The HOMO possesses an antibonding character between subunits, which may explain the nonplanarity observed for these oligomers in their ground state. On the other hand, the LUMO shows bonding character between the two adjacent rings, in agreement with the more planar S_1 excited state. Our calculated results indicate that all the carbazole-based polymers improve the hole injection due to the higher HOMO levels and the lower IPs, compared with those of conventional polyfluorene materials. Importantly, the charge carriers thiophene ring and ethynylene significantly lower the LUMO energies and consequently increase the EAs, which contribute to the highly improved electron-accepting and transporting properties. These two points are both essential for light-emitting polymers, and provide the opportunity of tuning the electronic and optical properties of the resulting polymers. On the other hand, our calculated results also indicate that the enhancement of the chain planarity will reduce the band gaps of carbazole-based copolymers, and vice versa.

Finally, this theoretical study confirmed experimental results where it was shown that by modification of chemical structures could greatly modulate and improve the electronic and optical properties of pristine polymers. Furthermore, using theoretical methodologies, we showed that is possible to predict reasonably the electronic properties of conjugated systems and we are convinced that the systematic use of those theoretical tools should contribute to orientate the synthesis efforts and help understand the structure–properties relation of these conjugated materials.

Acknowledgements

This work is supported by the Major State Basis Research Development Program (No. 2002CB 613406).

References

[1] Mitschke U, Bäuerle P. J Mater Chem 2000;10:1471.
[2] Kraft A, Grimsdale ACG, Holmes AB. Angew Chem, Int Ed 1998;37:402.
[3] Bernius MT, Inbasekaran M, O'Brien J, Wu W. Adv Mater 2000;12:1737.
[4] Leclerc M. J Polym Sci, Part A: Polym Chem 2001;39:2867.
[5] Lu JP, Tao Y, D'Iorio M, Li YN, Ding JF, Day M. Macromolecules 2004;37:2442.
[6] Beaupré S, Leclerc M. Macromolecules 2003;36:8986.
[7] Neher D. Macromol Rapid Commun 2001;22:1365.
[8] Cho NS, Hwang DH, Lee JI, Jung BJ, Shim HK. Macromolecules 2002;35:1224.
[9] Ego C, Marsitzky D, Becker S, Zhang J, Grimsdale AC, Müllen K, et al. J Am Chem Soc 2003;125:437.
[10] (a) Klärner G, Lee JI, Lee VY, Chan E, Chen JP, Nelson A, et al. Chem Mater 1999;11:1800.
(b) Lee JI, Klärner G, Miller RD. Chem Mater 1999;11:1083.
(c) Setayesh S, Grimsdale AC, Well T, Enkelmann V, Müllen K, Meghdadi F, et al. J Am Chem Soc 2001;123:946.
[11] (a) List EJW, Guentner R, Freitas PS, Scherf U. Adv Mater 2002;14:374.
(b) Lupton JM, Craig MR, Meijer EW. Appl Phys Lett 2002;80:4489.
[12] Yan H, Huang QL, Cui J, Veinot JGC, Kern MM, Marks T. Adv Mater 2003;15:835.
[13] (a) Morin JF, Leclerc M. Macromolecules 2001;34:4680.
(b) Morin JF, Leclerc M. Macromolecules 2002;35:8413.
[14] Zotti G, Schiavon G, Zecchin S, Morin JF, Leclerc M. Macromolecules 2002;35:2122.
[15] Belletête M, Bouchard J, Leclerc M, Durocher G. Macromolecules 2005;38:880.
[16] Lahti PM, Obrzut J, Karasz FE. Macromolecules 1987;20:2023–6.
[17] Zhang J-P, Frenking G. J Phys Chem A 2004;108:10296–301.
[18] Briére J-F, Côté M. J Phys Chem B 2004;108:3123–9.
[19] Brébdas J-L, Silbey R, Boudreaux D-S, Chance R-R. J Am Chem Soc 1983;105:6555–9.
[20] Ford W-K, Duke C-B, Paton A. J Chem Phys 1982;77(9):4564–72.
[21] Klaerner G, Miller RD. Macromolecules 1998;31:2007–9.
[22] Brébdas J-L, Chance R-R, Silbey R. Phys Rev B 1982;26:5843–54.
[23] Ma J, Li S-H, Jiang Y-S. Macromolecules 2002;35:1109–15.
[24] Zhang G-L, Ma J, Jiang Y-S. Macromolecules 2003;36:2130–40.
[25] Cao H, Ma J, Zhang G-L, Jiang Y-S. Macromolecules 2005;38:1123–30.
[26] Zhou X, Ren A-M, Feng J-K. Polymer 2004;7747–57.
[27] Wang JF, Feng JK, Ren AM, Liu XD, Ma YG, Lu P, et al. Macromolecules 2004;37:3451.
[28] Frisch MJ, Trucks GW, Schlegel HB, Scuseria GE, Robb MA, Cheeseman JR, et al. GAUSSIAN 03, Revision B.04. Pittsburg PA: Gaussian, Inc.; 2003.
[29] Gao Y, Liu C, Jiang Y. J Phys Chem A 2002;106:5380.
[30] Cornil J, Gueli I, Dkhissi A, Sancho-Garcia JC, Hennebicq E, Calbert J, et al. J Chem Phys 2003;118:6615–23.
[31] Ford WK, Duke CB, Salaneck WR. J Chem Phys 1982;77:5030.
[32] (a) Yang L, Ren AM, Feng JK, Liu XD, Ma YG, Zhang HX. Inorg Chem 2004;43:5961.
(b) Yang L, Ren AM, Feng JK, Ma YG, Zhang M, Liu XD, et al. J Phys Chem 2004;108:6797.
(c) Yang L, Ren AM, Feng JK. J Comput Chem 2005;26:969.
[33] De Oliveira MA, Duarte HA, Pernaut JM, De Almeida WB. J Phys Chem A 2000;104:8256–62.
[34] Hay PJ. J Phys Chem A 2002;106:1634–41.
[35] Curioni A, Andreoni W, Treusch R, Himpsel FJ, Haskal E, Seidler P, et al. J Appl Phys Lett 1998;72:1575–7.
[36] Hong SY, Kim DY, Kim CY, Hoffmann R. Macromolecules 2001;34:6474–81.
[37] Puschning P, Ambrosch-Draxl C, Heimel G, Zojer E, Resel R, Leising G, et al. Synth Met 2001;116:327.
[38] Eaton VJ, Steele D. J Chem Soc; Faraday Trans 1973;2:1601.